2024 IEEE International Conference on Robotics and Automation (ICRA 2024)
May 13-17, 2024. Yokohama, Japan

A Novel Compact Design of a Lever-Cam based Variable Stiffness Actuator: LC-VSA

Hongxi Zhu and Ulrike Thomas

Abstract— **Ensuring safe interaction between humans and robots is an important challenge in robotics. In recent years, researchers have developed many different soft robots. One possibility to reach this goal is to integrate mechanical springs into their joints. The forthcoming generation of soft robots will be adaptable for joint stiffness to accommodate various tasks. Consequently, the development of variable stiffness joints (VSA) has become crucial. Among the prevalent approaches for stiffness adjustment, lever mechanisms have been implemented in numerous variable stiffness joints. Nonetheless, the integration of the lever technology into VSA often faces challenges in achieving a compact design. This paper introduces a new mechanically compact design for a novel lever-cam based variable stiffness joint, which has been patent under the grand by the german Patentamt.**

I. INTRODUCTION

Safe interactions between robots and humans constitute a popular research field, with a significant demand for innovative solutions. To achieve this, researchers have developed joints with active compliance and passive compliance. Active compliant robot joints are often implemented as a joint-torque control loop to change the stiffnesses, which can be seen as a software based technology. Some robots on the market have successfully applied active compliance control, such as the robot IIWA by the manufacture KUKA or the robot Panda by Franka Emika. Because of the delay in the sensor acquisition data and the bandwidth of control loop, the performance of active compliance is limited. To address these limitations, passive compliance has been developed, employing mechanically elastic components. These mechanically elastic joints are capable of storing potential energy from impacts. However, the introduction of elastic components also results in increased instability. Control requirements for passive compliant technologies are significantly higher compared to active compliant technologies, which explains why robot arms with passive compliance are still undergoing extensive study.

Over the past decade, numerous researchers have proposed various designs for mechanical elastic joints, which can be categorized into two primary types: serial elastic actuators (SEAs) and variable stiffness actuators (VSAs). SEAs consist solely of springs positioned between the motor and the load, resulting in characteristic traits of being lightweight, compact, and maintaining a constant stiffness. Several SEAs have been developed by researchers, as evidenced by references [1], [2], [3], and [4]. This technology has also found practical application in commercially available robots such as Baxter. However, due to their fixed stiffness, SEAs encounter limitations in adapting to diverse tasks. To address this drawback, researchers have introduced VSAs, which incorporate an additional motor to enable the adjustment of joint stiffness. Researchers at the German Aerospace Center (DLR) have developed three VSA prototypes: the Floating Spring Joint [5], the VS-Joint [6], and the QA-Joint [7]. These prototypes utilize cam technology to achieve a progressive torque curve and prevent the joint from reaching mechanical limits. The cam-based VSAs employ a preload approach to adjust stiffness. Additionally, other VSAs, such as those mentioned in references [8] and [9], are also based on cam technology. Another popular method for adjusting stiffness is the lever mechanism. Researchers at the Italian Institute of Technology have developed three VSAs (AwAs [10], AwAs-II [11], and CompactArt-VSA [12]) that modify joint stiffness by manipulating the pivot point of the lever. Lever-based flexible joints typically exhibit approximately linear stiffness characteristics. However, due to their more intricate structure compared to cams, designing a compact form can often be challenging. Additionally, several other VSAs [13], [14], [15] also rely on the lever principle. Other VSAs [16] [17] [18], developed at the Italian Institute of Technology, employ a four-bar mechanism and torsion springs to achieve a progressive stiffness curve. In a different approach, the VSA described in [19] adopts a bidirectional antagonistic design and boasts cost-effective manufacturability. Furthermore, numerous researchers have employed leaf springs to devise VSAs [20] [21] [22] [23], adjusting stiffness by altering the effective length of the spring. At the University of Tokyo, researchers have taken this concept a step further, developing an advanced type of stiffness control module [24] that can be integrated into the body of a musculoskeletal humanoid robot.

In the past, we had developed a variable stiffness actuator [25], which combines a lever and a cam disc. However, the internal structure of old generation of VSA is not compact enough. Compared to the size of the actuator, the maximum torque performance is insufficient, hence it cannot be applied to a multi-joint manipulator. This paper describes a new soft joint, which uses a lever-cam based technique to realize a variable stiffness actuator (LC-VSA)(Fig. 1). The new actuator overcomes some disadvantages of previous VSAs. The new VSA has a high compact structure and can output more torque. The structure of this paper is as follows: the section II introduces the functional principle and the mechanical design. Section III describes the mathematical

All authors are with the Lab of Robotics and Human-Machine-Interaction, Chemnitz University of Technology, 09126, Chemnitz, Germany. Emails: {hongxi.zhu, ulrike.thomas}@etit.tu-chemnitz.de

model of the new VSA. Finally, conclusions and future work are discussed in section IV.

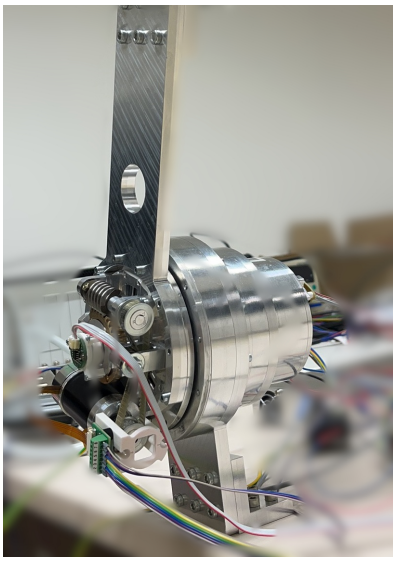

Fig. 1. The Lever-CAM based Variable Stiffness Actuator (LC-VSA).

II. Mechanical Design of the LC-VSA

In this section, we present the mechanical design and functional principles of the novel variable stiffness joint. This innovative joint amalgamates lever and cam technologies. The joint's stiffness can be adjusted by manipulating the pivot position of the levers, and a progressive torque curve is achieved through the utilization of a cam disc. Fig. 2 provides a visual representation of the new variable stiffness joint and offers insights into its dimensions. The maximum diameter of actuator is 130mm and the total length is 175mm. The weight of the actuator is 3.45kg. The right component in the figure denotes the actuator's output, which connects with the load. The mechanism for adjusting stiffness is affixed to the output.

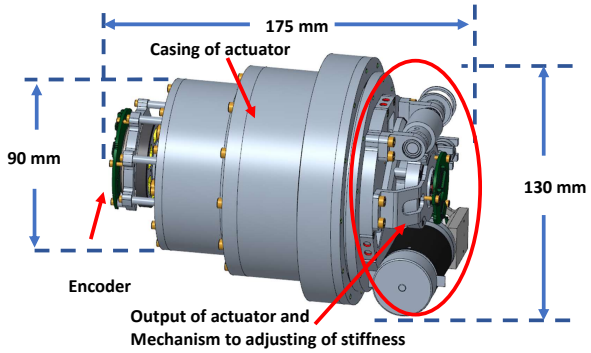

Fig. 2. The appearance of actuator.

The sectional view of the LC-VSA is illustrated in Fig. 3. The actuator can be divided into two main components: the first part comprises the traditional motor-gear system, while the second part is dedicated to the elastic mechanism module. The actuator incorporates a maxon EC frameless 60 flat motor, capable of generating a nominal torque of 319 mNm and a nominal speed of 3490 rpm. In Figure 3, the blue component represents the stator of the motor, securely affixed to the casing, while the green component corresponds to the rotor of the motor, which interfaces with the wave generator of the harmonic gear. An incremental encoder is mounted on the rotor to measure its speed. The actuator incorporates a harmonic gear CSD-25-2A with a $1:160$ ratio to amplify torque. Based on the gear's performance characteristics, the actuator is rated for a maximum torque output of 75Nm, which aligns with the gear's average torque capacity. The purple component represents the circular spline of the harmonic gear, connecting it to a shaft with an absolute encoder to measure the output position. In a traditional motor-gear system, the circular spline serves as the output of the actuator, directly connecting to the load. In the case of the elastic actuator, a cam disc is mounted on the circular spline, serving as the input to the elastic mechanism. The yellow component shows the module of the elastic mechanism.

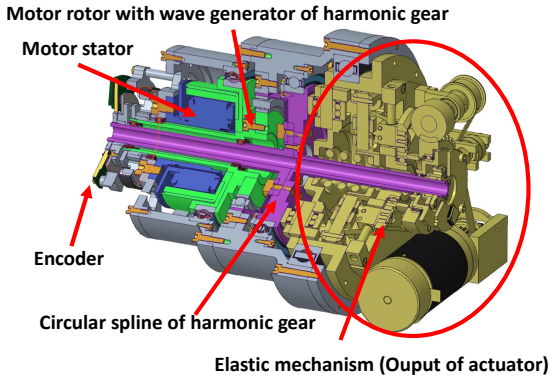

Fig. 3. The section of actuator.

The elastic mechanism module serves as the intermediary for transmitting torque from the output of the gear to the load through a lever-cam system. Fig. 4 (left) presents a sectional view of half of the elastic mechanism, showcasing one set of the lever-cam system. In our innovative design, three sets of lever-cam systems are utilized. The white component represents the cam disc, which interfaces with the circular spline of the harmonic gear as the input. The cam disc drives the yellow cam roller, which is mounted on the lower component (purple) of the mechanism. This lower component has the capability to move up and down along a guide within the casing of the elastic mechanism. A spring (orange) is positioned in the middle of the mechanism, located between the lower component (purple) and the upper component (blue). The green component represents the lever, with one side connecting to the upper component and the other to the lower component. The external torque applied to the mechanism is absorbed by the spring through the lever. A movable pivot (red) is mounted on the casing of the elastic mechanism. The pivot's position can be adjusted using a worm gear mechanism, as illustrated in Fig. 11 and 13. When an external load is imposed on the mechanism's

output, the lever-cam system undergoes deformation. Figure 4 (right) visually demonstrates the deformation of the elastic mechanism, with the lower component moving upward due to the cam action and the upper component moving downward due to leverage. This results in the compression of the spring by both the upper and lower components.

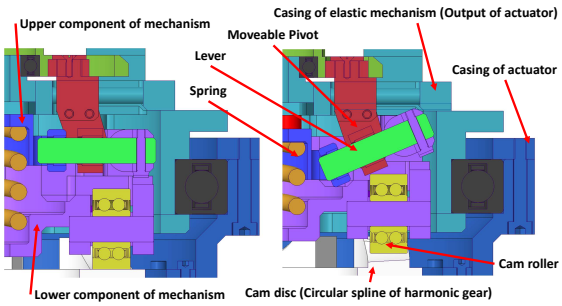

Fig. 4. The section of the elastic mechanism with standard stiffness. The left picture shows the mechnics in the rest position, and the right picture shows the deformation state

Fig. 5 present the sectional view of the elastic mechanism with the casing (left) and the top view without the casing (right), revealing the internal structure of the mechanism. The elastic mechanism comprises both upper and lower components. In comparison to other single-lever-based Variable Stiffness Actuators (VSAs), our design incorporates three sets of centrally symmetrical levers and cam rollers, resulting in a more compact structure and uniform force transmission. Six linear bearings are mounted on the lower component, allowing the elastic mechanism to slide along guides mounted on the casing.

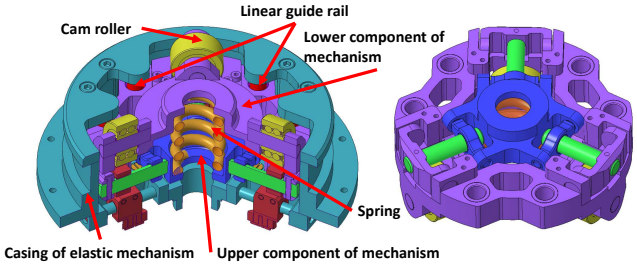

Fig. 5. The appearance of the elastic mechanism: (left) bottom view of the elastic mechanism with casing, (right) top view of the elastic mechanism without casing.

The cam disc, depicted in Fig. 6, divides and transmits the output torque of the harmonic drive through three cams, ensuring that each lever transmits a smaller force, thus allowing for smaller lever sizes. This design optimization enables a more compact overall design. Additionally, while other lever-based joints typically require at least two springs to absorb shocks in both positive and negative directions, our novel design only necessitates a single spring.

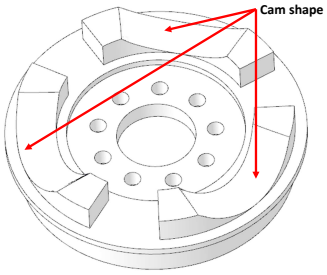

Fig. 6. The apperance of the cam disc.

Three movable pivot components are employed to adjust the stiffness. The position of the pivot is controlled by a slotted disc, as depicted in Fig. 7. When the disc rotates, the pivot component adjusts its position, thereby altering the stiffness of the system. The image in Fig. 7 on the left illustrates the VSA in a soft state, while the picture on the right depicts the VSA in a hard state.

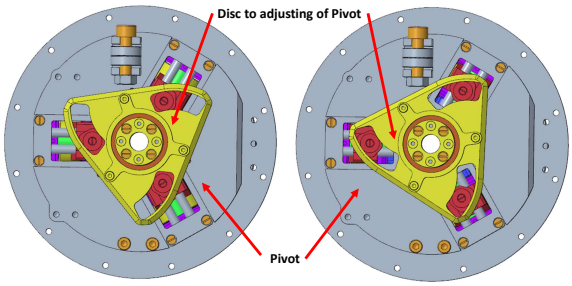

Fig. 7. The mechanism to adjusting of stiffness.

Fig. 8 left displays the sectional view of the mechanism when the stiffness is set to hard. In this configuration, the lever arm at the point of the lower component is shorter, and a small rotation of the cam disc can induce significant deformation of the spring. Fig. 8 right shows the deformation state with a high stiffness setting.

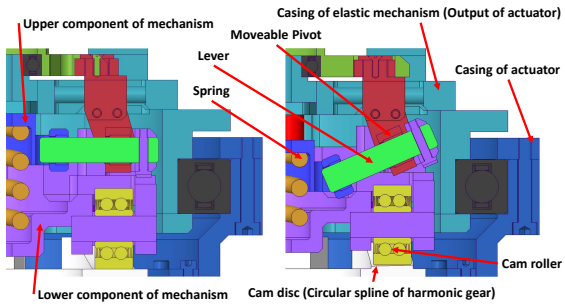

Fig. 8. The section view of the mechanism with a high stiffness. The left picture shows the mechnics in the rest position, and the right picture shows the deformation state

To drive the disc to adjusting of stiffness, we have incorporated an additional motor, a worm gear system, and a timing belt mechanism, as depicted in Fig. 9. Specifically, a maxon motor EC 32 flat with a planetary gear setup is mounted on the casing. A worm gear is securely fixed to the disc. The motor drives the worm via a timing belt.

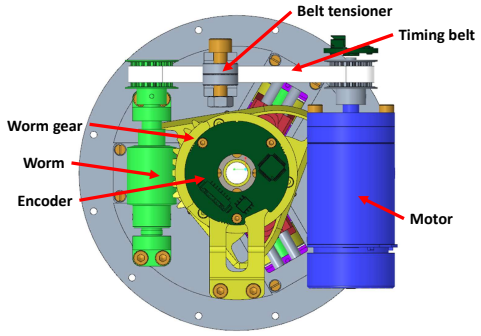

Fig. 9. The mechanism to adjusting of stiffness.

III. Mathematical Modelling

In this section, the functional principle of LC-VSA is discribed and the mathematical model of the variable stiffness actuator and the design of the cam shape is discussed. Fig. 10 depicts the functional principle of the mechanism in a relaxed state, while Fig. 11 presents the mechanism in a compressed state. It can be found from the pictures, that the force inside of the mechanism can be divided into horizontal and vertical forces due to the cam disc. The vertical forces are transmitted to the spring by the lever. The horizontal forces is transmitted to the casing of the elastic mechanism by three sets of linear bearings and produce the torque on the output. The three sets of linear bearings can only move along the guide, where the elastic mechanism can only move up and down in the casing, but it cannot rotate.

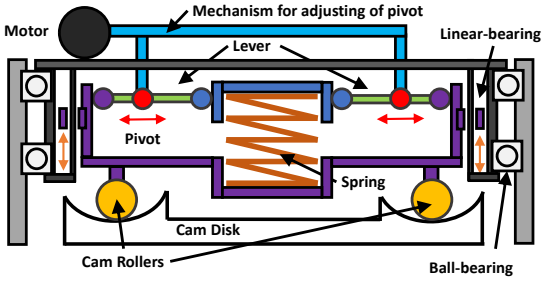

Fig. 10. The function principle of the elastic mechanism in a relaxed state.

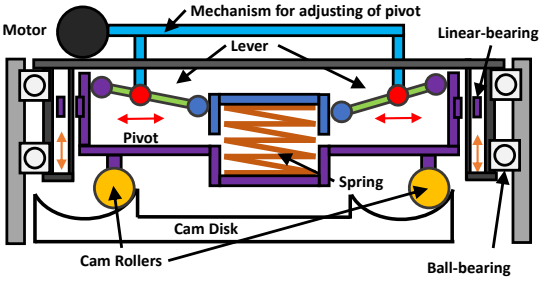

Fig. 11. The function principle of the elastic mechanism in a compressed state.

To create the model of the VSA, the model of the lever must be discussed firstly. Fig. 12 shows the force analysis diagram of a lever mechanism. The lever pivot divides the lever into two segments of length a and b. The variable y_1 is the upward movement of the lower component from the equilibrium position and y_2 is the downward movement of the upper component. F_s is the force of spring. F_l is the force, which is applied on the purple side of the lever. F_{vr} and F_{hr} are the vertical and horizontal force on the cam roller. r is is the distance between the cam roller and center of VSA.

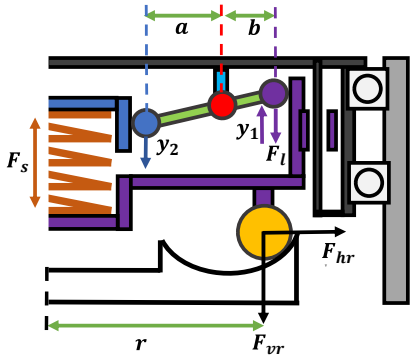

Fig. 12. Force analysis diagram of a lever mechanism.

The movement of the lower component, denoted as y_1, is determined by the cam shape, which we will discuss later. For the purposes of modeling the leverage, we assume that y_1 is a known parameter. The lever model elucidates the relationship between the input y_1 and the output torque τ. Leveraging this principle, the movement of the upper component can be calculated as follows:

$$y_2 = \frac{a}{b} y_1. \tag{1}$$

Since the spring is simultaneously deformed by both the upper and lower components, the deformation of the spring, denoted as y_s, is equal to the sum of y_1 and y_2.

$$y_s = y_1 + y_2 = \frac{a+b}{b} y_1. \tag{2}$$

The force F_s generated by the spring is

$$F_s = k_s y_s = k_s \frac{a+b}{b} y_1. \tag{3}$$

Here, k_s represents the spring constant. The spring force also affects both the upper and lower components. The force applied to the upper component will be transmitted to the purple end of the lever through the principle of leverage. This force, denoted as F_l, on the purple end of the lever can be calculated by

$$F_l = \frac{a}{b} F_s. \tag{4}$$

The vertical force F_{vr} exerted on the cam roller is equal to the sum of the spring force F_s applied to the lower component and the lever force F_l at the purple end of the lever.

$$F_{vr} = F_s + F_l = \frac{a+b}{b} F_s. \tag{5}$$

It is assumed, that the slope of the tangent at the contact point between the cam roller and the cam disc is k_t. The

horizontal force exerted on the cam disc can be calculated as follows:

$$F_{hr} = k_t F_{vr}. \tag{6}$$

The horizontal force generates torque, and this torque is equal to

$$\tau = F_{hr} r. \tag{7}$$

From equations (3) to (7). the model of lever can be written as

$$\tau = k_t k_s \frac{(a+b)^2}{b^2} y_1 r. \tag{8}$$

Next, the design of the cam shape is discussed. In this paper, a cubic Bézier curve is used to define the cam shape, as illustrated in Fig. 13. A Bézier curve is a special curve constructed using a starting point $\boldsymbol{P}_0$, an ending point $\boldsymbol{P}_3$, and control points $\boldsymbol{P}_1$ and $\boldsymbol{P}_2$. For a cubic Bézier curve, two control points are required to define the curve.

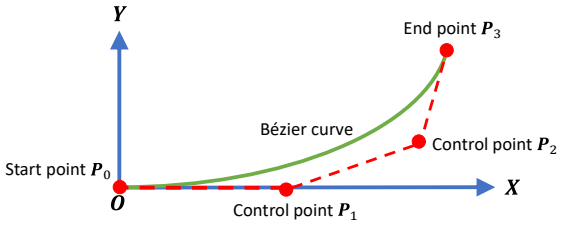

Fig. 13. Bezier curve to define the cam shape.

The function to define the cubic Bézier curve is

$$\begin{aligned}\begin{bmatrix} x(t) \\ y(t) \end{bmatrix} =& (1-t)^3 \boldsymbol{P}_0 + 3t(1-t)^2 \boldsymbol{P}_1 + 3t^2(1-t)\boldsymbol{P}_2 \\ &+ t^3 \boldsymbol{P}_3 \quad and \quad 0 \le t \le 1.\end{aligned} \tag{9}$$

The starting point $\boldsymbol{P}_0$ coincides with the origin. To maintain a tangent slope of 0 at the origin, the control point $\boldsymbol{P}_1$ must be situated on the x-axis. The position of the end point $\boldsymbol{P}_3$ along the x-axis is determined by the range of motion of the elastic mechanism. For our design, the elastic mechanism can rotate between -15° and 15°. The position of the end point $\boldsymbol{P}_3$ along the y-axis is determined by the maximum deformation of the spring. To calculate the tangent slope k_3 at point $\boldsymbol{P}_3$ based on the value of $\boldsymbol{P}_3$ and the designed maximum torque, we use equation (8). To ensure that the tangent slope at point $\boldsymbol{P}_3$ is maintained, the control point $\boldsymbol{P}_2$ must lie on the tangent line to $\boldsymbol{P}_3$. Therefore,

$$\begin{aligned}\boldsymbol{P}_0 = \begin{bmatrix} 0 \\ 0 \end{bmatrix}, \boldsymbol{P}_1 = \begin{bmatrix} x_1 \\ 0 \end{bmatrix}, \\ \boldsymbol{P}_2 = \begin{bmatrix} x_2 \\ k_3(x_2 - x_3) + y_3 \end{bmatrix}, \boldsymbol{P}_3 = \begin{bmatrix} x_3 \\ y_3 \end{bmatrix}.\end{aligned} \tag{10}$$

The variables x_3 and y_3 are known. By selecting appropriate variables x_1 and x_2, we can calculate the cam shape. Compared to other progressive curves (e.g., exponential functions or splines), the Bézier curve allows us to optimize only two variables. To model the VSA, we need to establish the relationship between x and y. We expand equation (9) and rearrange it to derive a new equation.

$$\begin{aligned}\begin{bmatrix} x(t) \\ y(t) \end{bmatrix} &= \boldsymbol{a}t^3 + \boldsymbol{b}t^2 + \boldsymbol{c}t \\ \boldsymbol{a} &= 3\boldsymbol{P}_1 - 3\boldsymbol{P}_2 + \boldsymbol{P}_3 \\ \boldsymbol{b} &= -6\boldsymbol{P}_1 + 3\boldsymbol{P}_2 \\ \boldsymbol{c} &= 3\boldsymbol{P}_1\end{aligned} \tag{11}$$

This forms a system of cubic equations. When x is known, we can calculate $t(x)$. By substituting $t(x)$ into the equation for y, we can determine the value of y. The relationship between x and y can only be described as an implicit function. When combined with the cam model and the lever model, we can obtain the model of the VSA. We choose

$$\boldsymbol{P}_1 = \begin{bmatrix} 4.22 \\ 0 \end{bmatrix}, \boldsymbol{P}_2 = \begin{bmatrix} 2.556 \\ 7 \end{bmatrix}, \boldsymbol{P}_3 = \begin{bmatrix} 7.854 \\ 3.41 \end{bmatrix}, \tag{12}$$

which can produce 4.45Nm at 5 degrees, 21.35Nm at 10 degrees, and 75.07Nm at 15 degrees. The cam shape is shown in Fig. 14.

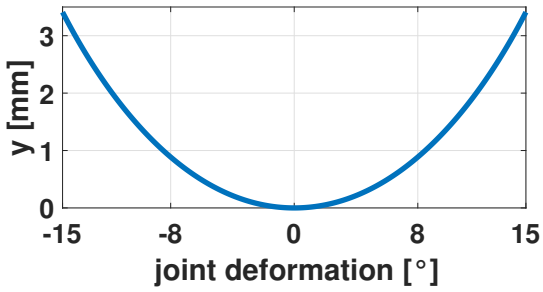

Fig. 14. Cam shape.

Fig. 15 and Fig. 16 shows the torque and stiffness curves of VSA. The variable b is the length of lever arm, which is shown in Fig. 12. The shorter the length b of lever arm is, the higher stiffness of VSA is.

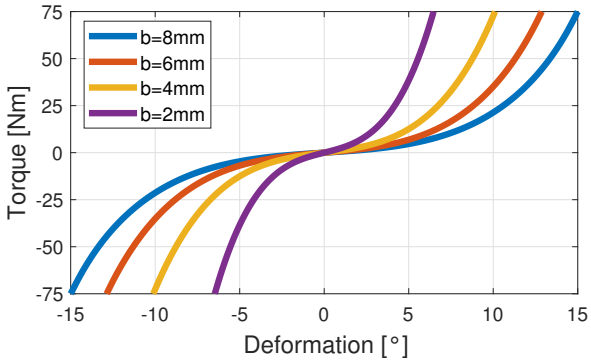

Fig. 15. The torque curve of VSA.

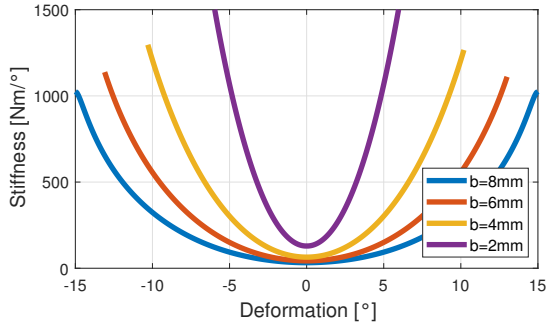

Fig. 16. The stiffness curve of VSA.

IV. Experiment and Results

To assess the performance of this new variable stiffness joint, an experiment was conducted. In this experiment, various torques were applied to the joint until the maximum deflection range was reached. Torque measurements were taken using a maxon controller, which calculates torque based on the current. Torques were measured at four different stiffness adjustments ($b = [2\text{ mm}, 4\text{ mm}, 6\text{ mm}, 8\text{ mm}]$).

Fig. 17 presents the results of the torque performance. It is evident that the motor produces 72 Nm of torque when the joint angle reaches 15 degrees. The torque curve closely mirrors the model curve, with minor disparities between the actual joint and the model curve, which can be attributed to manufacturing issues with the cam disc.

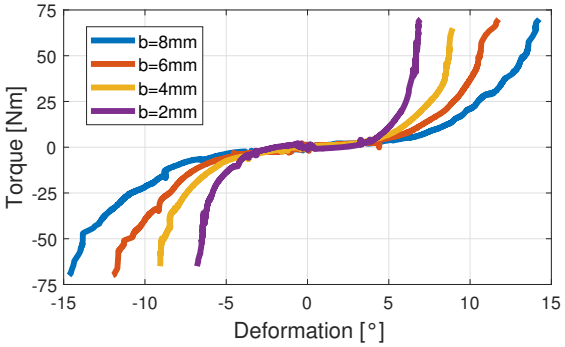

Fig. 17. Torque curve of VSA.

V. Conclusion and Future Work

This paper introduces the mechanical design and the model of a new variable stiffness actuator LC-VSA. This new joint is based on a novel combination of the lever and the cam-techniques to achieve a compact structure. The stiffness of the joint can be adjusted by manipulating the pivot position, and a desired progressive torque curve is achieved by a optimized shape of the cam disc. A robot with two such actuators will be built. In the future, the dynamic model of this elastic robot will be identified, and a model-based control strategy to control the elastic robot will be investigated.

References

[1] N. Paine, J. Mehling, J. Holley, N. A. Radford, G. Johnson, C.-L. Fok, and L. Sentis, "Actuator control for the nasa-jsc valkyrie humanoid robot: A decoupled dynamics approach for torque control of series elastic robots," *J. Field Robotics*, vol. 32, pp. 378–396, 2015.

[2] A. A. C. T. F. J. C. M. J. Tani and R. D. S. Guerra, "Dimitri: A low-cost compliant humanoid torso designed for cognitive robotics research," in *2016 XIII Latin American Robotics Symposium and IV Brazilian Robotics Symposium (LARS/SBR)*, Oct 2016, pp. 67–72.

[3] J. P. Cummings, D. Ruiken, E. L. Wilkinson, M. W. Lanighan, R. Grupen, and F. Sup IV, "A compact, modular series elastic actuator," vol. 8, 03 2016.

[4] J. Park and J. Song, "Safe joint mechanism using inclined link with springs for collision safety and positioning accuracy of a robot arm," in *2010 IEEE International Conference on Robotics and Automation*, May 2010, pp. 813–818.

[5] S. Wolf, O. Eiberger, and G. Hirzinger, "The dlr fsj: Energy based design of a variable stiffness joint," in *2011 IEEE International Conference on Robotics and Automation*, May 2011, pp. 5082–5089.

[6] S. Wolf and G. Hirzinger, "A new variable stiffness design: Matching requirements of the next robot generation," in *2008 IEEE International Conference on Robotics and Automation*, May 2008, pp. 1741–1746.

[7] O. Eiberger, S. Haddadin, M. Weis, A. Albu-Schäffer, and G. Hirzinger, "On joint design with intrinsic variable compliance: derivation of the dlr qa-joint," *2010 IEEE International Conference on Robotics and Automation*, pp. 1687–1694, 2010.

[8] B. Vanderborght, N. G. Tsagarakis, C. Semini, R. V. Ham, and D. G. Caldwell, "Maccepa 2.0: Adjustable compliant actuator with stiffening characteristic for energy efficient hopping," *2009 IEEE International Conference on Robotics and Automation*, pp. 544–549, 2009.

[9] F. Petit, W. Friedl, H. Höppner, and M. Grebenstein, "Analysis and synthesis of the bidirectional antagonistic variable stiffness mechanism," *IEEE/ASME Transactions on Mechatronics*, vol. 20, no. 2, pp. 684–695, April 2015.

[10] A. Jafari, N. G. Tsagarakis, and D. G. Caldwell, "A novel intrinsically energy efficient actuator with adjustable stiffness (awas)," *IEEE/ASME Transactions on Mechatronics*, vol. 18, no. 1, pp. 355–365, Feb 2013.

[11] ——, "Awas-ii: A new actuator with adjustable stiffness based on the novel principle of adaptable pivot point and variable lever ratio," in *2011 IEEE International Conference on Robotics and Automation*, May 2011, pp. 4638–4643.

[12] N. G. Tsagarakis, I. Sardellitti, and D. G. Caldwell, "A new variable stiffness actuator (compact-vsa): Design and modelling," *2011 IEEE/RSJ International Conference on Intelligent Robots and Systems*, pp. 378–383, 2011.

[13] P. Yin, M. Li, W. Guo, P. Wang, and L. Sun, "Design of a unidirectional joint with adjustable stiffness for energy efficient hopping leg," in *2013 IEEE International Conference on Robotics and Biomimetics (ROBIO)*, Dec 2013, pp. 2587–2592.

[14] S. S. Groothuis, G. Rusticelli, A. Zucchelli, S. Stramigioli, and R. Carloni, "The variable stiffness actuator vsaut-ii: Mechanical design, modeling, and identification," *IEEE/ASME Transactions on Mechatronics*, vol. 19, no. 2, pp. 589–597, April 2014.

[15] M. Dežman and A. Gams, "Pseudo-linear variable lever variable stiffness actuator: Design and evaluation," in *2017 IEEE International Conference on Advanced Intelligent Mechatronics (AIM)*, July 2017, pp. 785–790.

[16] R. Schiavi, G. Grioli, S. Sen, and A. Bicchi, "Vsa-ii: a novel prototype of variable stiffness actuator for safe and performing robots interacting with humans," in *2008 IEEE International Conference on Robotics and Automation*, May 2008, pp. 2171–2176.

[17] M. G. Catalano, G. Grioli, F. Bonomo, R. Schiavi, and A. Bicchi, "Vsa-hd: From the enumeration analysis to the prototypical implementation," in *2010 IEEE/RSJ International Conference on Intelligent Robots and Systems*, Oct 2010, pp. 3676–3681.

[18] M. G. Catalano, R. Schiavi, and A. Bicchi, "Mechanism design for variable stiffness actuation based on enumeration and analysis of performance," in *2010 IEEE International Conference on Robotics and Automation*, May 2010, pp. 3285–3291.

[19] M. G. Catalano, G. Grioli, M. Garabini, F. Bonomo, M. Mancini, N. Tsagarakis, and A. Bicchi, "Vsa-cubebot: A modular variable stiffness platform for multiple degrees of freedom robots," in *2011 IEEE International Conference on Robotics and Automation*, May 2011, pp. 5090–5095.

[20] J. Choi, S. Hong, W. Lee, S. Kang, and M. Kim, "A robot joint with variable stiffness using leaf springs," *IEEE Transactions on Robotics*, vol. 27, no. 2, pp. 229–238, April 2011.

[21] Y. Tao, T. Wang, Y. Wang, L. Guo, H. Xiong, and F. Chen, "Design and modeling of a new variable stiffness robot joint," in *2014 International Conference on Multisensor Fusion and Information Integration for Intelligent Systems (MFI)*, Sept 2014, pp. 1–5.

[22] G. A. Naselli, L. Rimassa, M. Zoppi, and R. Molfino, "A variable stiffness joint with superelastic material," *Meccanica*, vol. 52, no. 4, pp. 781–793, Mar 2017. [Online]. Available: https://doi.org/10.1007/s11012-016-0423-1

[23] V. Chalvet and D. J. Braun, "Algorithmic design of low-power variable-stiffness mechanisms," *IEEE Transactions on Robotics*, vol. 33, pp. 1508–1515, 2017.

[24] O. Masahiko, I. Nobuyuki, N. Yuto, and I. Masayuki, "Stiffness readout in musculo-skeletal humanoid robot by using rotary potentiometer," in *SENSORS, 2010 IEEE*, Nov 2010, pp. 2329–2333.

[25] H. Zhu and U. Thomas, "A new design of a variable stiffness joint," in *2019 IEEE/ASME International Conference on Advanced Intelligent Mechatronics (AIM)*, 2019, pp. 223–228.